

DIAGNOSIS AND QUANTITATIVE ASSESSMENT OF MANDIBULAR ASYMMETRY USING CBCT IMAGE VOLUMES

Abeer AlHadidi, BDS

A thesis submitted to the faculty of the University of North Carolina at Chapel Hill in partial fulfillment of the requirements for the degree of Master of Science in the school of Dentistry, (Oral and maxillofacial radiology).

Chapel Hill

2010

Approved by:

Advisor: Lucia Cevidanes DDS,
PhD

Reader: John Ludlow DDS, Msc

Reader: Andre Mol DDS, PhD

ABSTRACT

Abeer AlHadidi: Diagnosis and quantitative assessment of mandibular asymmetry
using CBCT image volumes

(Under the direction of Lucia Cevidanes)

Objectives: To compare two methods of measuring mandibular asymmetry. The first method uses mirroring of the mandible in the midsagittal plane; the second uses arbitrary mirroring of the mandible and registration on the cranial base. **Methods:** Surface models were constructed from CBCT scans of 50 patients with asymmetry. For the first approach, a midsagittal plane was defined for each patient as the plane passing through Nasion, ANS, and Basion. Mirrors for both halves of the mandible were created. The second approach was to mirror each model on an arbitrary plane. Both original and arbitrarily mirrored images were registered on the cranial base. Surface distances between hemimandibles and mirrors were calculated for nine regions. **Results:** There was no statistically significant difference between the mean surface distance measurements obtained with the two approaches, and comparing both halves in most areas. **Conclusion:** Both mirroring techniques provided similar quantification of mandibular asymmetry in this cohort.

ACKNOWLEDGEMENTS

In recognition of their time and effort in making this project possible, I would like to thank the members of my committee: Drs. Cevidanes, Ludlow, and Mol, particularly Dr. Cevidanes for her enthusiasm and amazing energy. I would like to thank Beatriz Paniagua for the time and effort she put in the project. I would also like to thank Mom and Dad, my family, and my best friends Sandra, Sahar, and Ammar for always being there.

TABLE OF CONTENTS

I.	List of Figures	vi
II.	List of tables	viii
III.	Manuscript 1	1
	A. Introduction.....	1
	B. Materials and methods.....	2
	C. Results.....	4
	D. Discussion.....	5
	E. Conclusion.....	7
	F. References.....	8
IV.	Manuscript 2	10
	A. Abstract.....	10
	B. Introduction	12

C. Materials and methods.....	13
D. Results.....	17
E. Discussion.....	18
F. Conclusion.....	20
G. References.....	21

LIST OF FIGURES

Figure 1. Assessment of asymmetry following two different mirroring methods.....	24
Figure 2. A Box plot demonstrating the mean of the absolute difference in surface distance measurements (mm) using both mirroring methods on each ROI on the Left side	24
Figure 3. A Box plot demonstrating the mean of the absolute difference in surface distance measurements (mm) using both mirroring methods on each ROI on the right side	25
Figure 4. A Box plot demonstrating the mean of the absolute difference in surface distance measurements (mm) of the left and right sides of the mandible using mirroring on the midsagittal plan.	26
Figure 5. A Box plot showing the mean of the absolute difference in surface distance measurements (mm) of the left and right sides of the mandible using arbitrary mirroring followed by registration on the cranial base	27
Figure 6. Examples of patients with challenging asymmetries for quantification.....	28
Figure 7. Validation of asymmetry quantification methods.....	29
Figure 8. Image segmentation.....	30
Figure 9. Three-dimensional image mirroring on the midsagittal plane	31
Figure 10. Arbitrary plane mirroring followed by cranial base registration approach.....	32
Figure 11. Asymmetry simulation.....	33
Figure 12. Description of shape correspondence procedures.....	34
Figure 13. Quantification of mandibular asymmetry for a patient using Shape Correspondence.....	35
Figure 14. Examples of yaw in mandibular asymmetry.....	36
Figure 15. Clinical case 1.....	37

Figure 16. Clinical case 2.....38

Figure 17. Clinical case 3.....39

LIST OF TABLES

Table 1. Descriptive statistics for the absolute difference in surface distance measurements between the two methods at the different anatomical locations.....	40
Table 2. The probabilities, confidence intervals and prediction intervals for x, y, and z rotation and translation as measured for simulated asymmetries using mirroring in the midsagittal plane.....	41
Table 3. The probabilities, confidence intervals and prediction intervals for each x, y z possible planes of rotation and translation measured for the simulated asymmetries for the arbitrary mirroring/cranial base registrations approach.....	42

Manuscript 1

Introduction

Facial asymmetry is common and sometimes poses a challenge in craniofacial diagnosis and treatment planning.^{1, 2} It is etiologically and pathologically heterogeneous and may be localized or generalized. This wide variability in the etiology and in the presentation of the disease necessitates that the management of those patients be a multifactorial stepwise decision making process. Proper assessment and quantification of the differences between the right and the left sides are crucial for diagnosis, treatment planning and follow up. Conventional postero-anterior cephalometric radiographs used in orthodontic practice to assess asymmetry have inherent limitations as a result of superimposition, magnification and distortion.

Three dimensional imaging (3D) and associated image analysis methods developed recently carry a potential for development in this field. The use of relatively low dose cone beam computed tomography (CBCT) scanners in dental practice facilitates the examination of anatomical structures in a multi-planar view. It also provides a rich soil for the application of different image analysis techniques to further extract diagnostic information from available volumes. Creation of 3D virtual surface models from CBCT volumes, registration of those models, and measurements of the surface distances between different models is a

well documented approach used to study growth, treatment changes, and the stability of those changes.³⁻⁷

Various approaches have been described in the literature in an attempt to use 3D imaging for detection and quantification of craniofacial asymmetry.⁸⁻¹⁰ However, most of these techniques depend on landmark identification and manual identification of a straight “midsagittal plane” both of which proved to be extremely challenging and operator dependent.

In 2000, a method to automatically define the midsagittal plane of the brain in 2D cross-sectional slices was presented.¹¹ However, definition of the midsagittal plane in the maxillofacial area remains a challenge because the plane is a curved surface in some faces with chin deviation. In 2004, an alternative method for determining a symmetry plane was presented, using mirroring of the mandible in any arbitrary plane with rigid registration of the mirrored mandible to the original image.¹² However, this procedure did not take into consideration the mandibular morphologic relationships with the maxilla and the cranial base. A modification of this approach, that first mirrors the image and then registers on the cranial base, can provide information on the entire facial structure rather than just the mandible.⁷

The aim of this study was to compare the degree of mandibular asymmetry, as obtained by surface distance measurement, using *mirroring of the mandible in the “midsagittal plane”* vs. *arbitrary mirroring of the mandible and registration on the cranial base*.

Materials and methods

Following a protocol approved by the institutional review board for research involving human subjects, fifty patients with clinically detectable asymmetry served as the cohort of this study. Clinical asymmetry was defined as more than 2 mm of chin deviation or the presence of cant of the occlusal plan before the start of their orthodontic treatment. CBCT scans of all patients were obtained using NewTom 3G cone beam scanner (Aperio Services, Sarasota, Fla). The 12” field of view producing 0.5 mm isotropic voxel sizes was used for acquiring the image volume. Three-dimensional surface models were constructed from the CBCT volumes using segmentation tools of the Insight SNAP software.¹³ Following segmentation, a 3D graphical rendering of the volumetric object allows navigation between voxels in the volumetric image and the 3D graphics with zooming, rotating and panning.

Mid-Sagittal Plane Approach

Nasion (Na), Anterior Nasal Spine (ANS), and Basion (Ba) were manually defined for each patient by one observer. The midsagittal plane was defined as the plane passing through those three landmarks. The resultant midsagittal plane was used to create mirrors for both halves of the mandible.

Na, ANS, Ba, the midsagittal plane and the degree of asymmetry were determined five times on 22 randomly selected patients from the cohort. Differences between repeated assessments of asymmetry served as a measure of reproducibility of midsagittal plane identification.

Arbitrary Plane plus Registration Approach

Each model was mirrored on an arbitrary plane. The original and the arbitrarily mirrored images were then registered on the cranial base.

CMFApp software^{14, 15-17} was used to display the superimposed images with the two approaches: (1) Original image superimposed on image *mirrored* on the *midsagittal plane*; and (2) Original image superimposed on image *mirrored* on an *arbitrary plane*, and then *registered to the original image*.

Surface distances were compared between the resultant mirrors from both approaches and the original mandible. The average surface distances of the right and left side were calculated for nine anatomical regions: the lateral pole, medial pole, anterior and posterior surfaces of both condyles, lateral surface of the rami and corpora of the mandible, inferior and posterior surfaces of the mandible, and anterior surface of the symphysis. The measures of surface distances were complemented by visualization of the 3-D color coded maps (Fig 1)

Paired T tests were used to assess statistical differences between the surface distance measurements obtained by the two approaches for each anatomical location. They were also used to test for differences between the measurements obtained for the right and the left sides for each approach. The Cochran-Mantel-Haenszel test was used to test for the effect of the degree of asymmetry on the difference detected between the two approaches ($\alpha= 0.05$).

Results

The variability in surface distance measurements obtained from five repeated assessments of the midsagittal plane for each subject ranged from 0 to 1.63 mm with a mean of 0.42 mm

and a standard deviation of 0.18 mm. Only 5 patients had a discrepancy larger than 1mm. The paired t-tests showed no statistically significant difference in quantification of asymmetry among the five measurement sets ($p > 0.1$ for all paired comparisons, and $p = 0.44$ when pooled measurements were tested together).

Of the 18 anatomical areas measured, the mandibular ramus ($p = 0.04$), body ($p = 0.01$), and symphysis ($p = 0.005$) at the right side and the lateral pole of the condyle at the left side ($p = 0.02$) showed statistically significant differences in the mean surface distance between the two approaches. The differences in the mean surface distances ranged from 0.2 to 1.5 mm. (Fig 2-3)

A positive correlation between asymmetry measurements and the discrepancy between the methods was observed at the right inferior border ($p=0.048$), left posterior border ($p=0.04$), and medial pole of left condyle ($p=0.03$).

There was no statistically significant difference in the mean of surface distance measurements between the left and the right side for all locations using the registered mirror. However, a significant difference was observed in the ramus ($p=0.02$), the body of the mandible ($p=0.03$), and the symphysis area ($p=0.04$) when mirroring with the midsagittal plane was used. (Fig 4-5)

Discussion

Although cephalometric radiography has been, and will probably continue to be, the routine radiographic examination for any patient seeking orthodontic\orthognathic treatment, the “inappropriateness of conventional cephalometrics” has been recognized as early as 1979.¹⁸ Those inadequacies are further accentuated when challenged with bilateral

differences in the anatomy. 3D cephalometry has the potential advantage of being able to better detect and localize existing asymmetries. However, quantification of asymmetries using 3D cephalometry heavily depends on the operator's understanding of 3D landmark definition and the ability to reproducibly define those landmarks.^{8,9} The use of surface distance measurements between the two halves of the mandible that served as our asymmetry quantification outcome overcomes the need to depend on points as surrogates for real structures.

In this cohort, the use of either mirroring approach (midsagittal plane and an arbitrary plane with registration on the cranial base) provided similar results in most areas. Most of the discrepancies in surface distance measurements were located on the lateral surface of the mandible, which suggests that the medio-lateral direction is most sensitive to mirroring.

It can be hypothesized that there should be no difference in the absolute surface distance measurements based on whether the right or the left side of the mandible is being mirrored. That was true when mirroring using an arbitrary plane with registration on the cranial base, but the use of a midsagittal plane mirroring produced inconsistencies at some locations. It follows that most of those locations were the same ones that showed discrepancies between the two approaches.

The differences between the two mirroring approaches, though statistically insignificant, tended to increase with more severe asymmetries. Application of both approaches to an exclusive cohort of patients with severe asymmetries may further characterize this trend in terms of location and the cut-off point of maximal difference.

Neither approach could be applied indiscriminately to any patient. Mirroring using the midsagittal plane is difficult for patients suffering from conditions that interfere with the

midline position of the points used to define the midsagittal plane, i.e., cleft palate patients. On the other hand, registration on the cranial base in patients with asymmetries involving the cranial base would also result in suboptimal results.

Applying both mirroring approaches to patients with rudimentary condyles, severe cants, or a rotated mandible would result in a mirror image that is not aligned to the original. This complicates the interpretation of the surface distances obtained at a specified location. The measured distance would not represent the difference between corresponding anatomical locations, but rather the minimal difference between the models as computed by the Iterative Closest Point algorithm used by CMF. (Fig 6)

Conclusion

In conclusion, both mirroring using a midsagittal plane and using an arbitrary plane followed by registration on the cranial base provided similar quantification of mandibular asymmetry for most areas. One of these approaches is considered an alternative to the other when certain structural features of the patient impede the use of either approach.

Shape correspondence, a technology that allows measuring the surface distance between an area on one model to the same corresponding area in the other model regardless of the alignment of those models, is currently being investigated as a promising alternative to overcome the shortcomings of the iterative closest point algorithm.

References

1. Severt TR, Proffit WR. The prevalence of facial asymmetry in the dentofacial deformities population at the university of north carolina. *Int J Adult Orthodon Orthognath Surg.* 1997;12(3):171-6.
2. Proffit WR, Fields HW, Jr, Moray LJ. Prevalence of malocclusion and orthodontic treatment need in the united states: Estimates from the NHANES III survey. *Int J Adult Orthodon Orthognath Surg.* 1998;13(2):97-106.
3. Cevidanes LH, Bailey LJ, Tucker GR, Jr, Styner MA, Mol A, Phillips CL, et al. Superimposition of 3D cone-beam CT models of orthognathic surgery patients. *Dentomaxillofac Radiol.* 2005 Nov;34(6):369-75.
4. Cevidanes LH, Bailey LJ, Tucker SF, Styner MA, Mol A, Phillips CL, et al. Three-dimensional cone-beam computed tomography for assessment of mandibular changes after orthognathic surgery. *Am J Orthod Dentofacial Orthop.* 2007 Jan;131(1):44-50.
5. Cevidanes LH, Franco AA, Gerig G, Proffit WR, Slice DE, Enlow DH, et al. Comparison of relative mandibular growth vectors with high-resolution 3-dimensional imaging. *Am J Orthod Dentofacial Orthop.* 2005 Jul;128(1):27-34.
6. Cevidanes LH, Franco AA, Gerig G, Proffit WR, Slice DE, Enlow DH, et al. Assessment of mandibular growth and response to orthopedic treatment with 3-dimensional magnetic resonance images. *Am J Orthod Dentofacial Orthop.* 2005 Jul;128(1):16-26.
7. Cevidanes LH, Styner MA, Proffit WR. Image analysis and superimposition of 3-dimensional cone-beam computed tomography models. *Am J Orthod Dentofacial Orthop.* 2006 May;129(5):611-8.
8. Katsumata A, Fujishita M, Maeda M, Arijji Y, Arijji E, Langlais RP. 3D-CT evaluation of facial asymmetry. *Oral Surg Oral Med Oral Pathol Oral Radiol Endod.* 2005 Feb;99(2):212-20.
9. Maeda M, Katsumata A, Arijji Y, Muramatsu A, Yoshida K, Goto S, et al. 3D-CT evaluation of facial asymmetry in patients with maxillofacial deformities. *Oral Surg Oral Med Oral Pathol Oral Radiol Endod.* 2006 Sep;102(3):382-90.
10. Park SH, Yu HS, Kim KD, Lee KJ, Baik HS. A proposal for a new analysis of craniofacial morphology by 3-dimensional computed tomography. *Am J Orthod Dentofacial Orthop.* 2006 May;129(5):600.e23,600.e34.
11. Prima S, Ourselin S, Ayache N. Computation of the mid-sagittal plane in 3D images of the brain. *Computer Vision & ECCV 2000.* 2000:685-701.

12. Nanna Glerup. Asymmetry measures in medical image analysis [dissertation]. Department of Innovation IT, University of Copenhagen; April 29, 2005.
13. Yushkevich PA , Piven J, Hazlett HC, Smith RG, Ho S, Gee JC, et al. User-guided 3D active contour segmentation of anatomical structures: Significantly improved efficiency and reliability. *NeuroImage*.2006;31 (3):1116-28.
14. Chapuis J. Computer- aided cranio-maxillofacial surgery [dissertation]. Switserland: University of Bern; 2006.
15. Chapuis J, Ryan P, Blaeuer M, Langlotz F, Hallermann W, Schramm A, et al. A new approach for 3D computer-assisted orthognathic surgery—first clinical case. *Int Congr Ser*. 2005 5;1281:1217-22.
16. De Momi EF, Chapuis JF, Pappas IF, Ferrigno GF, Hallermann WF, Schramm AF, et al. Automatic extraction of the mid-facial plane for cranio-maxillofacial surgery planning. *International journal of oral and maxillofacial surgery*. 2006;35(7):636-42.
17. Chapuis J , Rudolph T, Borgesson B, De Momi E, Pappas I, Hallermann W, Schramm A, et al. 3D surgical planning and navigation for CMF surgery .*SPIE Medical imaging*, San Diago, California, USA. 2004 February .
18. Moyers RE, Bookstein FL. The inappropriateness of conventional cephalometrics. *Am J Orthod* 1979 6;75(6):599-617

Manuscript 2

Abstract:

Objective: To determine if 3D shape correspondence can accurately quantify mandibular asymmetry in surgical patients. **Methods:** Pretreatment cone-Beam CT scans were acquired of twenty orthognathic surgery patients with different degrees and types of facial asymmetry. The maxillofacial hard tissues were segmented and mirroring was performed for virtual surgical planning using the CranioMaxilloFacial Application software. Mirrored surgical models were superimposed on the actual patient models using two different approaches: (1) mirroring on the midsagittal plane; and (2) mirroring on an arbitrary plane with registration on the cranial base. Different amounts of additional mandibular asymmetry in the three planes of space were simulated by known amounts. For both mirroring methods, SPHARM shape correspondence was used to detect and quantify simulated asymmetries. **Results** SPHARM-shape correspondence accurately quantified different types and degrees of virtually simulated facial asymmetry. The probabilities for all 6 degrees of freedom (rotation and translation) that the difference between asymmetry measurements and the known virtually simulated value is less than 0.5mm was very good for both mirroring techniques

on the midsagittal plane (probability 0.99 to 1) and mirroring on an arbitrary plane with cranial base registration (probability 0.84 to 1). For mandibular corpus asymmetries that cannot be masked by genioplasty, virtual simulation of the correction of mandibular tilt and rotations was required prior to quantification of mandibular asymmetry correction.

Conclusions: The detection and quantification of asymmetry allows the surgeon to localize and quantify left and right side differences. In addition, to the use of the midsagittal plane for mirroring the cranial base registration performs equally well and could be applied in difficult trauma situations or when key landmarks are unreliable or absent Future validation of maxillary, occlusal and soft tissue components of facial asymmetries will be valuable. Supported by NIDCR DE017727, DE018962, DE005215 and NCRR UL1RR025847.

Introduction

Software applications based on cone-beam computed tomography (CBCT) or spiral Computer tomography (CT) allow virtual preparation of the operative plan, however, precise knowledge of the location of the facial asymmetry plane is essential for the diagnosis of facial deformities and for the planning of corrective and reconstructive procedures.¹ The identification of a midsagittal plane allows correction of the head tilt in the image data and facilitates visual and quantitative assessment of asymmetry. In addition, the midsagittal plane can be used in asymmetrical deformities to mirror the healthy facial side.²

Mirroring is a technique which uses a mirrored image of the contralateral side as a reference for the diagnosis, preparation, or execution of asymmetric surgical displacements or unilateral reconstructions. This technique requires adequate definition of the symmetry plane used in the mirroring operation. The result can then be employed as a template for correction of the affected side. Several methods have been proposed to compute the midsagittal plane using volumetric image datasets.²⁻⁶ Previous work on a landmark-based midsagittal plane showed that the definition of the midsagittal plane is sufficiently reliable.⁷ A second method, based on mirroring the mandible in an arbitrary plane with rigid registering on the cranial base, also provides information of the mandibular asymmetry relative to the face.⁸

As 3D computer planning systems to assess mandibular asymmetry are increasingly used in clinical practice, it is important to validate the clinical application of these methods and critically assess the difficulty of quantifying asymmetry. The aim of this study was to determine if SPARM-shape correspondence based on segmented cone beam CT scans can

correctly detect and quantify mandibular asymmetry when two different mirroring techniques are used.

Materials and methods

Using twenty existing pretreatment CBCT scans, right and left mandibular morphology were compared by superimposing two image volumes. Patients ranged in age from 9 to 41 years with a mean age of 21 years. All subjects were taken from a consecutive prospectively collected sample that sought care at our dentofacial deformities program and consented to participate in the project. Patients were included if they had clinically detectable asymmetry, defined as more than 2 mm of chin deviation or the presence of cant of the occlusal plan before the start of their orthodontic treatment. Exclusion criteria were (1) history of previous jaw surgery and (2) reconstructive surgery with grafting.

Image acquisition- NewTom 3G Cone Beam CTs were obtained prior to orthodontic treatment.

Construction of virtual 3D models from the CBCT dataset. The first step in this process involved segmentation of hard tissues by outlining the shape of structures visible in the axial slices of the volumetric dataset. Segmentation of anatomic structures was performed with ITK-SNAP.⁹⁻¹⁰ 3D virtual models were built from a set of approximately 300 axial cross-sectional reformatted with an isotropic voxel size of 0.5 x 0.5 x 0.5 mm. Higher spatial resolution with smaller slice thickness would have increased image file size and would have required greater computational power and user interaction time. Following segmentation with ITK-SNAP, a 3D graphical rendering of the volumetric object allowed navigation between voxels in the image volume using zooming, rotating and panning. (Fig 8)

Mirroring approaches

Midsagittal Plane Approach

Nasion (Na), Anterior Nasal Spine (ANS), and Basion (Ba) were defined for each patient. The midsagittal plane was defined as the plane passing through those three landmarks. The resultant midsagittal plane was used to create mirrors for both halves of the mandible, creating right and left hemi-mandibles. (Fig 9)

The reliability of the observer to determine the midsagittal plane was assessed in a previous study: The midsagittal plane was identified 5 times on 22 randomly selected patients, and the differences in quantification of asymmetry served as a measure of reproducibility of midsagittal plane identification.⁷

Arbitrary Plane Mirroring followed by Cranial Base Registration Approach

Each virtual model was mirrored on an arbitrary plane. The original and the arbitrarily mirrored images were then registered on the cranial base. (Fig 10)

The CMF software was used to display the superimposed images with the two approaches: (1) Original image superimposed to *mirrored* image on the *midsagittal plane*; and (2) Original image superimposed to *mirrored* image on an *arbitrary plane*, and then *registered to original image*. A mutual-information based registration maps one image to another, using a rigid transform to evaluate within subject changes. This task was performed using the registration pipeline within the Imagine Software developed at UNC.¹¹ Our superimposition methods are fully automated, using voxel-wise rigid registration of the cranial base instead of the current standard landmark matching method, which is observer-

dependent and highly variable. After masking out maxillary and mandibular structures, the registration transform was computed solely on the grey level intensities in the cranial base. Rotation and translation parameters were calculated and then applied to register the 3D models.

Asymmetry simulation: Asymmetry simulation was performed with the CranioMaxilloFacial (CMF) software application. (M.E. Müller Institute for Surgical Technology and Biomechanics, University of Bern, Switzerland.) For each left and right hemimandible asymmetry was simulated by translating the original models, with a known value of added asymmetric displacement (1mm x, 2mm x, 3mm x, 1mm z, 2mm z, 3mm z, 1mm x 2mm z, 2mm x 1 mm z and 3mm x 3mm z, where x is a vertical and z is a lateral plane of translation).

Asymmetric lateral and superior-inferior simulated translational movements were performed to create additional asymmetries of known magnitude (1, 2 and 3mm simulations). Simulated asymmetries were performed on the three dimensional pretreatment models by a single examiner. After the virtual simulation of asymmetry, the mirror models were used to quantify the asymmetry and visualize the right and left side differences. This was done by changing the color and reducing the opacity of displaced models which were superimposed with the original mirror models. (Fig11).

Quantification of differences between simulated asymmetries and mirror models: Shape Correspondence (SC) was employed to provide a unique and symmetric point correspondence across all measured surfaces. The correspondence was computed by mapping every point on the mandibular 3D surface models to a unique position on the unit sphere

(SPHARM software, developed as part of the NAMIC consortium),¹² followed by generating a uniformly triangulated surface based on this spherical mapping (SPHARM-PDM).¹³ (Fig 12) Jaw asymmetry was measured for each right and left hemi-mandibles, comparing the original and the mirrored structures. First, subtraction of mirrored and original (actual) asymmetry models allowed a template for surgical corrections displaying color-coded corresponding distance maps and maps of vectors of differences between these models. Second, subtraction of mirror and simulated asymmetry models generated color-coded corresponding distance maps and maps of vectors of differences between these models. The distance maps measure the magnitude of the differences between the mirror and the simulated asymmetry point-based models, while the vector maps offer directionality (Fig 13). The six degrees of freedom (DOF) of the differences were calculated using rigid Procrustes alignment. The geometric transformation that best maps the shape changes between the mirror and simulated asymmetry point-based correspondent models measured asymmetry in six DOF. The measured simulated translations with Shape correspondence/Procrustes were the absolute differences between the measurements of simulated asymmetries and the actual asymmetries: ([procrustes between each simulation translated hemimandible and original mirrored hemimandible] - [procrustes between original hemimandible and original mirrored hemimandible]).

Statistics analysis: Three statistical methods were used to analyze the accuracy of asymmetry representation using SPHARM-PDM: (1) $P(|\bar{X} - known| < .5)$, the probability that the sample mean measurement was within 0.5mm (translation) or 5^0 (rotation) of the true value of the simulated asymmetry, (2) 95% confidence interval (CI), and (3) 95% prediction interval (PI). The 95% CI provides an interval with 95% confidence that the true mean falls

within the interval. The confidence interval doesn't necessarily contain the true mean. The 95% PI is an estimate of an interval that a future observation of a random variable is expected to fall within with a 95% probability. It can be considered as a "confidence interval" for prediction. The prediction interval is always wider than the confidence interval because of the additional uncertainty for prediction. All analyses were based on the assumption of a normal distribution for this population.

Clinical application of SPHARM- Shape correspondence to quantify mandibular asymmetry: After the validation study, SPHARM-shape correspondence was then applied as a diagnostic tool to aid treatment planning for asymmetric patients (Figures 14-17)

Results

Table 2 shows the results for the midsagittal plane mirroring and describes the probabilities, confidence intervals and prediction intervals for the x, y and z rotation and translation measured for the simulated asymmetries using mirroring in the midsagittal plane. Table 3 shows the results for the arbitrary mirroring with cranial base registration approach. The probability that the magnitude of the asymmetry measurement difference from the known value of simulated asymmetry was less than 0.5 mm of translation or 5⁰ of rotation was high for midsagittal plane mirroring (0.99-1) as well as for the arbitrary mirroring with cranial base registration (0.84-1). For this clinical application, measurements smaller than the voxel size of the image volume (0.5mm) were considered accurate. The results showed an acceptable error range in measurements calculated for both mirroring techniques with SPHARM-shape correspondence. All 95% confidence and probability intervals contained the hypothesized means (known asymmetry values, Tables 2 and 3).

SPHARM-Shape correspondence quantification of asymmetry. This procedure generated color maps visual displays of magnitude, direction, and location of disagreement between models. The clinical application of mirroring techniques and SPHARM-Shape correspondence to quantify mandibular asymmetry is illustrated in Figures 14-17.

Discussion

An increasing number of studies have demonstrated that Computer aided surgical simulation (CASS) has lower material costs as well as decreased surgical time, comparable or better surgical outcomes, reduced complications and increased predictability of surgical complications. It has also been utilized to allow more complex surgeries to be successfully performed in a single procedure rather than the previous multiple staged surgeries.^{4, 14-18} The ability to visualize facial asymmetry in 3D surface models does not imply the ability to quantify and precisely locate areas of asymmetry. Future benefits also include the fabrication of stereolithographic models and surgical splints, which have the potential to greatly reduce intra-operative time and surgical complications.¹⁶

In this study, the use of mirroring on the midsagittal plane allowed precise and reproducible measurements of asymmetry. However, the choice of landmarks used to determine the midsagittal plane might have a marked impact on the asymmetry quantification. Manual selection of landmarks is time-consuming, as it requires great care and attention during the selection process. In addition, the result depends on availability and visibility of the anatomical landmarks and on the ability of the user to identify them. In a particular face, symmetry is often better described by several regional symmetry axes (e.g., symmetry between jaw and midface regions often differs, for which no defining landmark set

exists).¹⁹ In severe asymmetries, as in craniofacial microsomia or cleft patients, entire regions of the anatomy might be missing or severely dislocated. In these cases selection of landmarks could result in an incorrect quantification of asymmetry.

The measurements calculated for arbitrary mirroring with cranial base registration had slightly lower probabilities compared to mirroring in the midsagittal plane. It did, however, had acceptable precision and could be used as an alternative assessment method, particularly for patients with marked mandibular asymmetry, but with relatively symmetric cranial base. The concept of a mirroring technique using arbitrary mirroring is possible by the subsequent voxel wise rigid registration of the cranial base. We have validated this method in previous studies.⁹ It has been shown to be more accurate than traditional landmark methods for three dimensional superimpositions.²⁰⁻²¹ The larger the number of points used for superimposition the more accurate it becomes. If the patient's cranial base is symmetric, the use of a stable and symmetric facial structure has proven to be a reliable reference for diagnosing the facial roll and yaw components of mandibular asymmetry.

Ackerman and Proffit emphasized that valid and reliable quantification of appearance continues to elude researchers.²² Interpretation of facial asymmetry even if in 3D by subjective visual assessment of right and left differences can lead to inadequate diagnosis and mislead treatment planning (Figure 14). They suggested that the labial intercommissure line and NHP are examples of orientations determined by soft tissues that should be used in the evaluation of transverse roll of the dentition.²³ However; the labial intercommissure line can be affected by muscular and facial animation asymmetries. In the past, the inability to appreciate the interplay between maxillomandibular roll and yaw was a missing link in classification and diagnosis. When one sees a major midline shift, a unilateral Class II or

Class III molar relationship, or a true unilateral crossbite, quantification of the mandibular roll and yaw is essential prior to the quantification of actual left and right differences²³ (Figures 16 and 17). The extent of asymmetric yaw is a major determinant in whether treatment is limited to asymmetric mechanics or might extend to asymmetric extractions, unilateral bone anchors, or surgery.²³

The assessments in this study were performed as a baseline diagnosis before orthodontic preparation. However, pretreatment diagnosis does not necessarily reflect the presurgical planning that might change depending on the orthodontics mechanics and correction of the dental midlines. The techniques validated in this study may be generalizable and can be applied for pre-surgical assessment as in Figure 16.

There has been a surge in recent years of commercially available programs for three dimensional virtual surgery and visualization programs.^{2-6, 25} The biggest drawback to these programs is the lack of validation. The results of this study demonstrate that facial asymmetry with six degrees of freedom can be accurately quantified. This rapidly developing technology may have a significant impact on future surgical procedures.

Conclusions

SPHARM-shape correspondence in combination with mirroring techniques allows visualization and quantification of the location, direction and magnitude of differences between right and left sides of the mandible. Future efforts should be directed towards validation of similar tools for other craniofacial skeletal components, the occlusion and the soft tissues.

References

1. O'Grady K, Antonyshyn O. Facial asymmetry: three-dimensional analysis using laser surface scanning. *Plast Reconstr Surg* 1999; 104: 928–937.
2. E. De Momi, J. Chapuis, I.P. Pappas, G. Ferrigno, W. Hallermann, A. Schramm, and M. Caversaccio. Automatic extraction of the mid-facial plane for cranio-maxillofacial surgery planning. *International Journal of Oral and Maxillofacial Surgery*, 2006.
3. Gellrich N, Schramm A, Hammer B, Rojas S, Cufi D, Lagreze W, Schmelzeisen R. Computer assisted secondary reconstruction of unilateral posttraumatic orbital deformity. *Plast Reconstr Surg* 2002; 110: 1417–1429.
4. Hassfeld S, Muhling J. Computer assisted oral and maxillofacial surgery--a review and an assessment of technology. *Int J Oral Maxillofac Surg*. 2001 Feb;30(1):2-13.
5. Junck L, Moen JG, Hutchins GD, Brown MB, Kuhl DE. Correlation methods for the centering, rotation and alignment of functional brain images. *J Nuclear Med* 1990; 3: 1220–1226.
6. Liu Y, Collins RT, Rothfus WE Robust midsagittal plane extraction from normal and pathological 3-D neuroradiology images. *IEEE Trans Med Imaging* 2001; 20: 175–192.
7. Alhadidi A, Cevidanes LHS, Mol A, Ludlow J, Styner MA. 3D Analysis of Facial Asymmetry based on Midsagittal Plane Computation. *J Dent Res*. 2009;88(Spec Issue A):311.
8. Cevidanes LH, Styner MA, Proffit WR. Image analysis and superimposition of 3-dimensional cone-beam computed tomography models. *Am J Orthod Dentofacial Orthop* 2006 May;129(5):611-8
9. Cevidanes LH, Bailey LJ, Tucker GR, Jr, Styner MA, Mol A, Phillips CL, et al. Superimposition of 3D cone-beam CT models of orthognathic surgery patients. *Dentomaxillofac Radiol*. 2005 Nov;34(6):369-75.
10. Yushkevich PA, Piven J, Hazlett HC, Smith RG, Ho S, Gee JC, et al. User-guided 3D active contour segmentation of anatomical structures: significantly improved efficiency and reliability. *Neuroimage*. 2006 Jul 1;31(3):1116-28.
11. Cevidanes LH, Bailey LJ, Tucker SF, Styner MA, Mol A, Phillips CL, et al. Three-dimensional cone-beam computed tomography for assessment of mandibular changes after orthognathic surgery. *Am J Orthod Dentofacial Orthop*. 2007 Jan;131(1):44-50.

12. Styner M, Oguz I, Xu S, Brechbuhler C, Pantazis D, Levitt J, et al. Framework for the statistical shape analysis of brain structures using SPHARM-PDM. Special edition open science workshop at MICCAI. *Insight J* 2006;1-7.
13. Gerig G, Styner M, Jones D, Weinberger D, Lieberman J. Shape analysis of brain ventricles using SPHARM. *MMBIA Proceedings. IEEE* 2001;171-8.
14. Xia J, Samman N, Yeung RW, Shen SG, Wang D, Ip HH, et al. Three-dimensional virtual reality surgical planning and simulation workbench for orthognathic surgery. *Int J Adult Orthodon Orthognath Surg.* 2000 Winter;15(4):265-82.
15. Gateno J, Teichgraeber JF, Xia JJ. Three-dimensional surgical planning for maxillary and midface distraction osteogenesis. *J Craniofac Surg.* 2003 Nov;14(6):833-9.
16. Gateno J, Xia JJ, Teichgraeber JF, Christensen AM, Lemoine JJ, Liebschner MA, et al. Clinical feasibility of computer-aided surgical simulation (CASS) in the treatment of complex cranio-maxillofacial deformities. *J Oral Maxillofac Surg.* 2007 Apr;65(4):728-34.
17. Xia J, Ip HH, Samman N, Wang D, Kot CS, Yeung RW, et al. Computer-assisted three-dimensional surgical planning and simulation: 3D virtual osteotomy. *Int J Oral Maxillofac Surg.* 2000 Feb;29(1):11-7.
18. Troulis MJ, Everett P, Seldin EB, Kikinis R, Kaban LB. Development of a three-dimensional treatment planning system based on computed tomographic data. *Int J Oral Maxillofac Surg.* 2002 Aug;31(4):349-57.
19. Tung-Yui W, Jing-Jing F, Tung-Chin W. A Novel Method of Quantifying Facial Asymmetry. H U Lemke, K Inamura, K Doi, M W Vannier, and A G Farman, editors, *Computer Assisted Radiology and Surgery*, Berlin, Germany. 2005 June.
20. Gliddon MJ, Xia JJ, Gateno J, Wong HT, Lasky RE, Teichgraeber JF, et al. The accuracy of cephalometric tracing superimposition. *J Oral Maxillofac Surg.* 2006 Feb;64(2):194-202.
21. Xia JJ. Accuracy of the computer-aided surgical simulation (CASS) system in the treatment of patients with complex craniomaxillofacial deformity: A pilot study. *Journal of oral and maxillofacial surgery.* 2007 -02;65(2):248-54.
22. Ackerman JL, Proffit WR. A not-so-tender trap. *Am J Orthod Dentofacial Orthop.* 2009 Nov;136(5):619-20
23. Ackerman JL, Proffit WR, Sarver DM, Ackerman MB, Kean MR. Pitch, roll, and yaw: describing the spatial orientation of dentofacial traits. *Am J Orthod Dentofacial Orthop.* 2007 Mar; 131(3):305-10.

24. Glerup, N. Nielsen, M. Sparring, J. Kreiborg, S. Asymmetry Quantization and Application to Human Mandibles. Journal title Proceedings- SPIE the international society for optical engineering VOL 5370; PART 1, pages 274-282 Publisher International Society for Optical Engineering; 1999.

Figure 1. Assessment of asymmetry following 2 different mirroring methods.

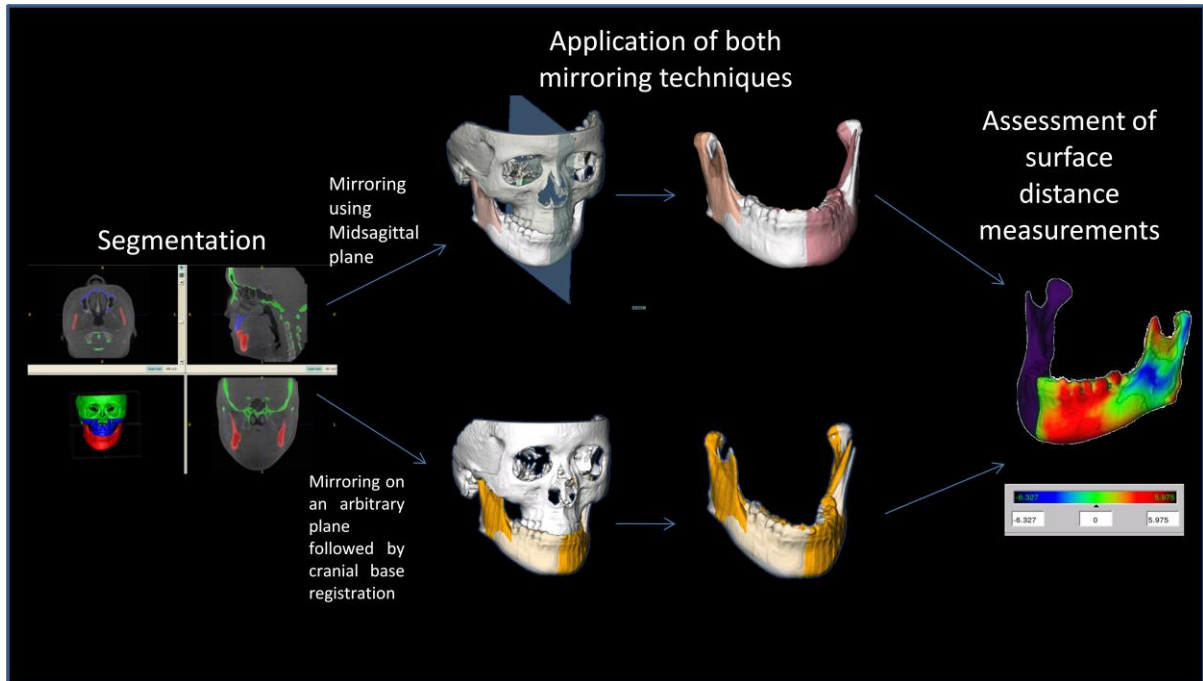


Figure 2. A Box plot demonstrating the mean of the absolute difference in surface distance measurements (mm) using both mirroring methods on each ROI on the Left side (* indicates statistical significance)

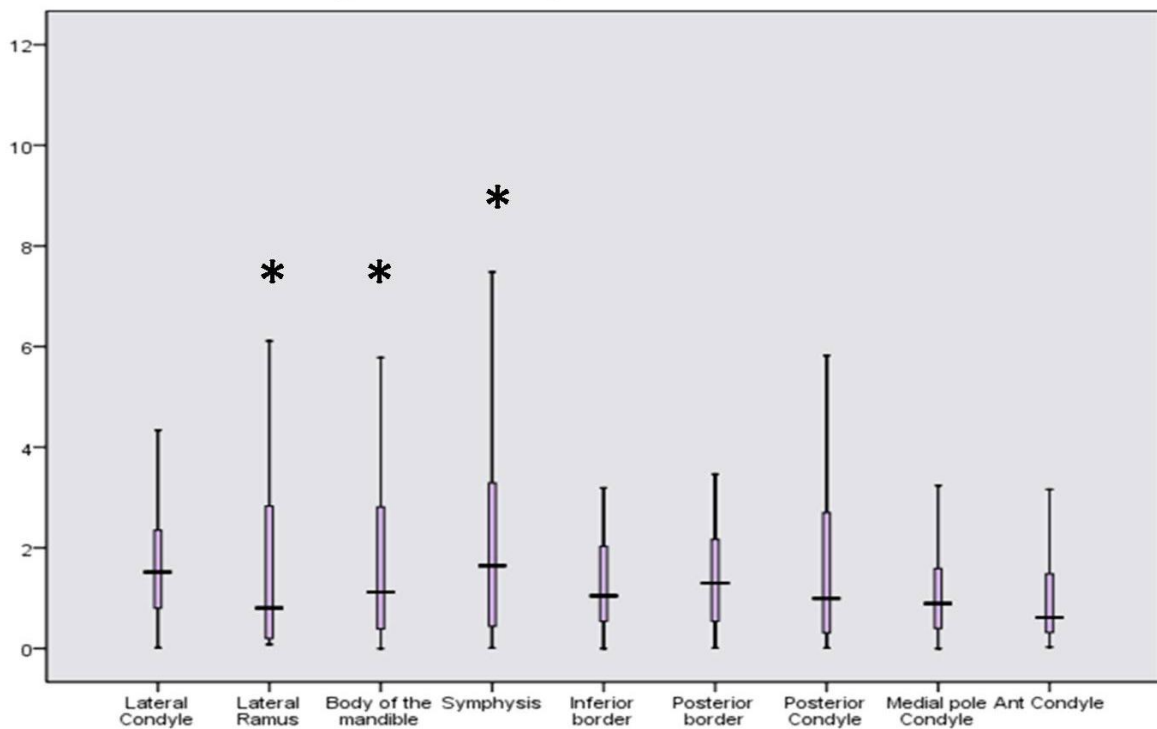


Figure 3. A Box plot demonstrating the mean of the absolute difference in surface distance measurements (mm) using both mirroring methods on each ROI on the right side (* indicates statistical significance)

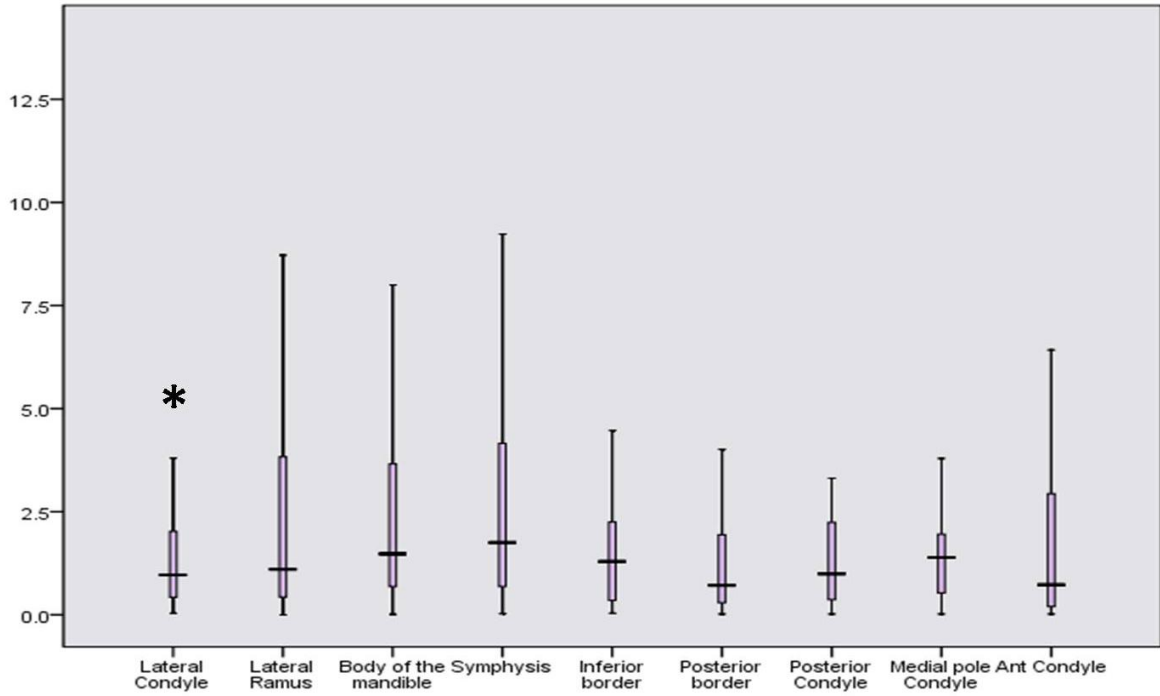


Figure 4. A Box plot showing the mean of the absolute difference in surface distance measurements (mm) of the left and right sides of the mandible using mirroring on the midsagittal plan. (* indicates statistical significance)

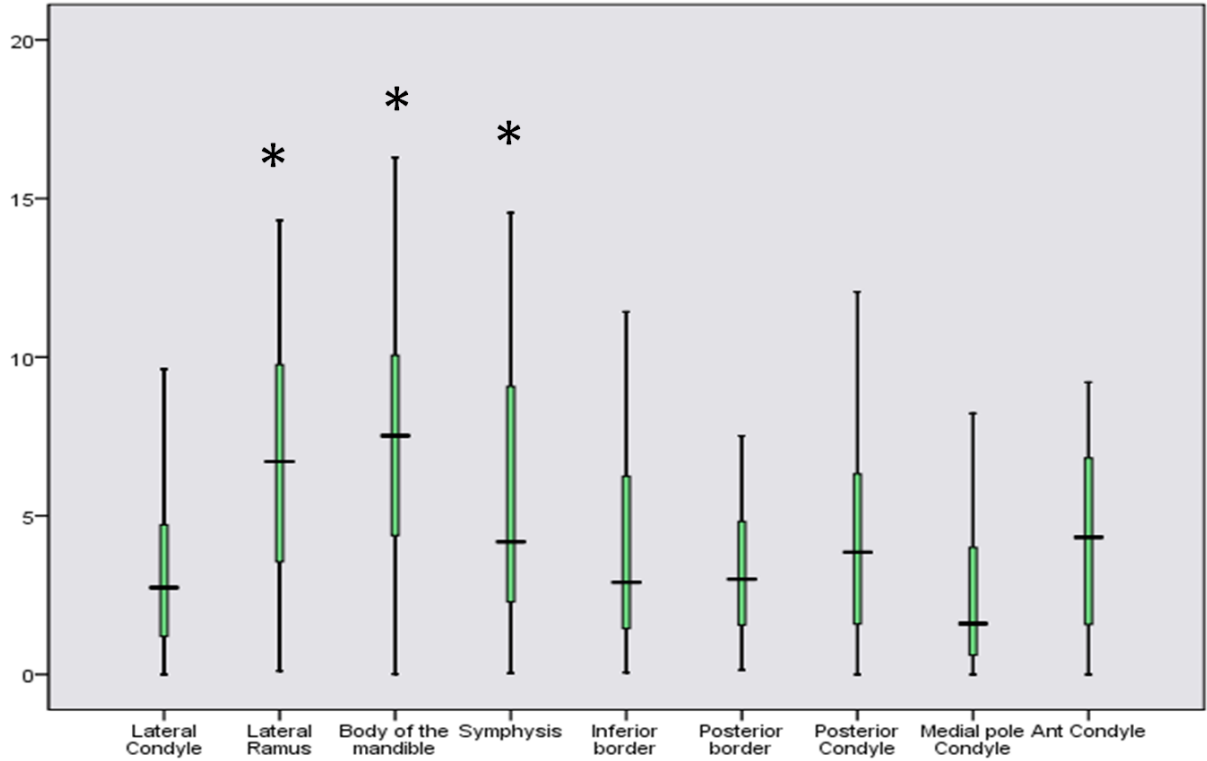


Figure 5. A Box plot showing the mean of the absolute difference in surface distance measurements (mm) of the left and right sides of the mandible using arbitrary mirroring followed by registration on cranial base

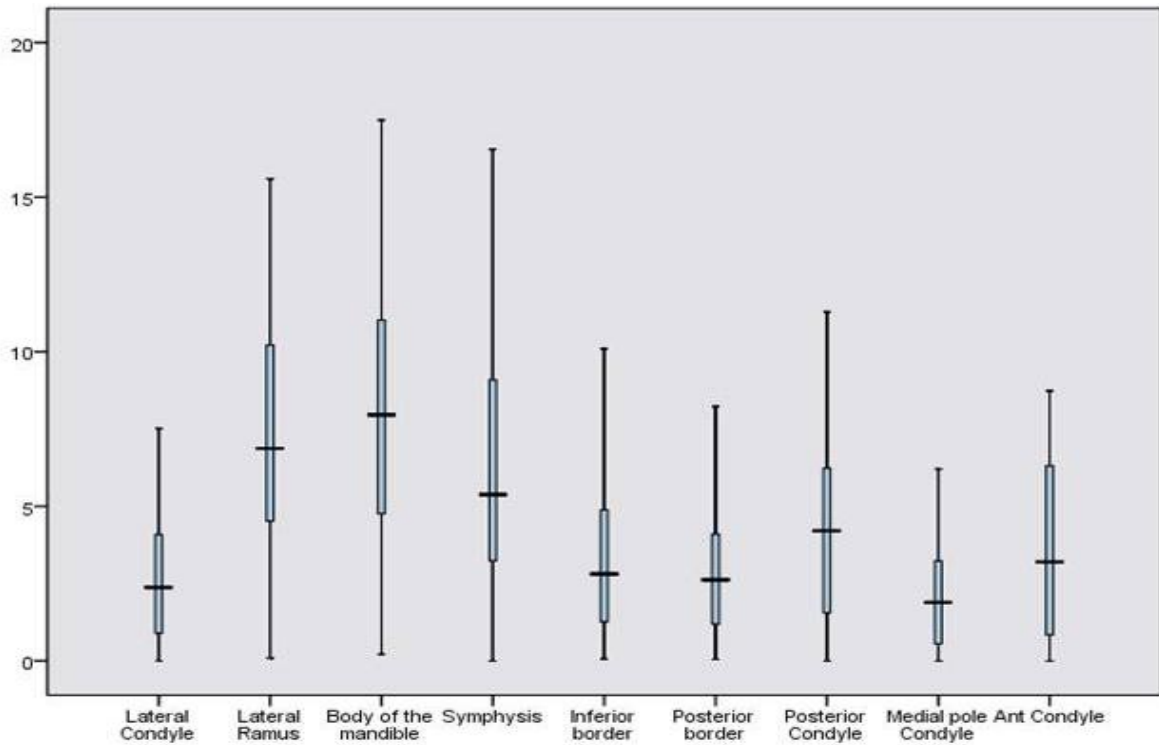


Figure 6. Examples of patients with challenging asymmetries for quantification. Asymmetric cranial base (A) and cleft palate (B) would interfere with both mirroring protocols. Severe cant (C) and rotation (D) is hard to deal with using ICP.

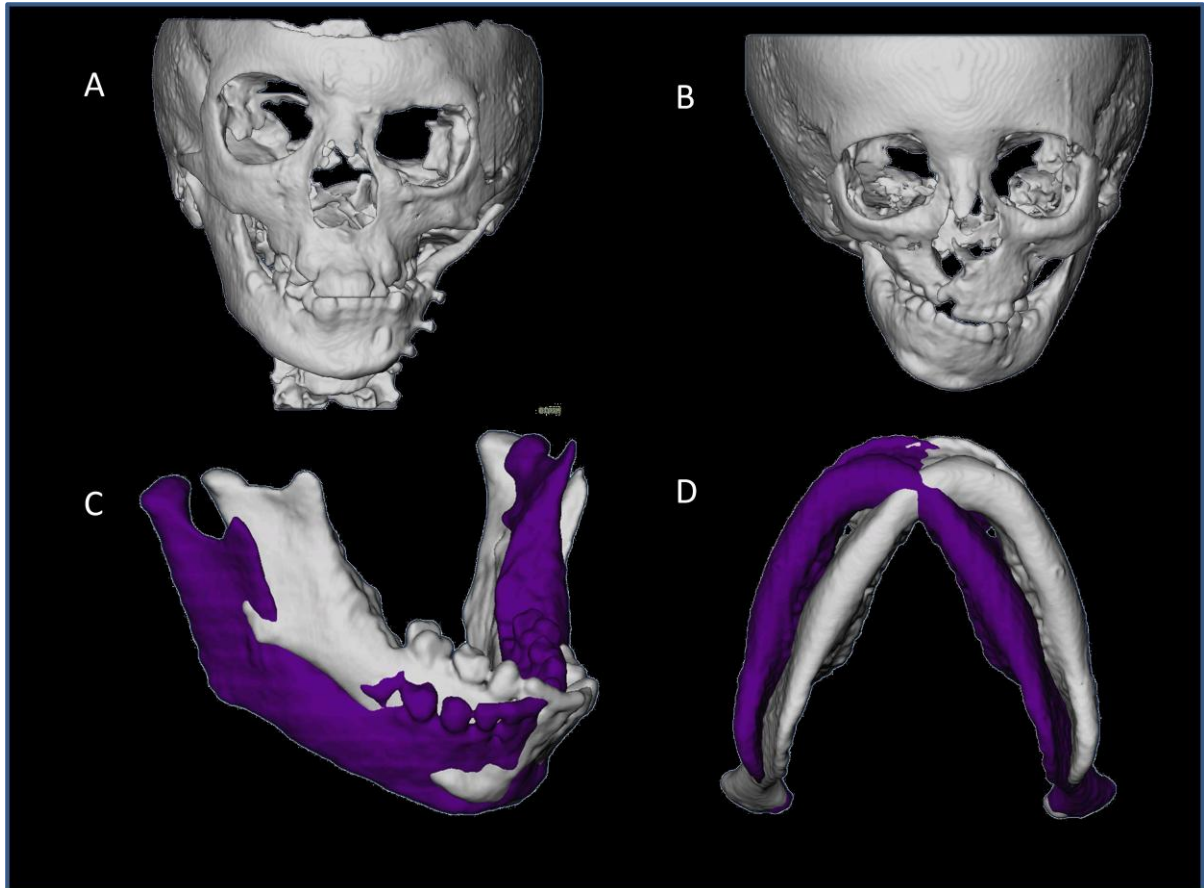


Figure 7. Validation of asymmetry quantification methods: (1) Cone beam CT's are taken for each patient and segmentation involves delineation of the anatomical areas of interest. (2) Visualization of the two mirroring techniques used to create mirror images for quantification of right and left side differences. (3) Simulation of asymmetry (4) Quantification of asymmetry.

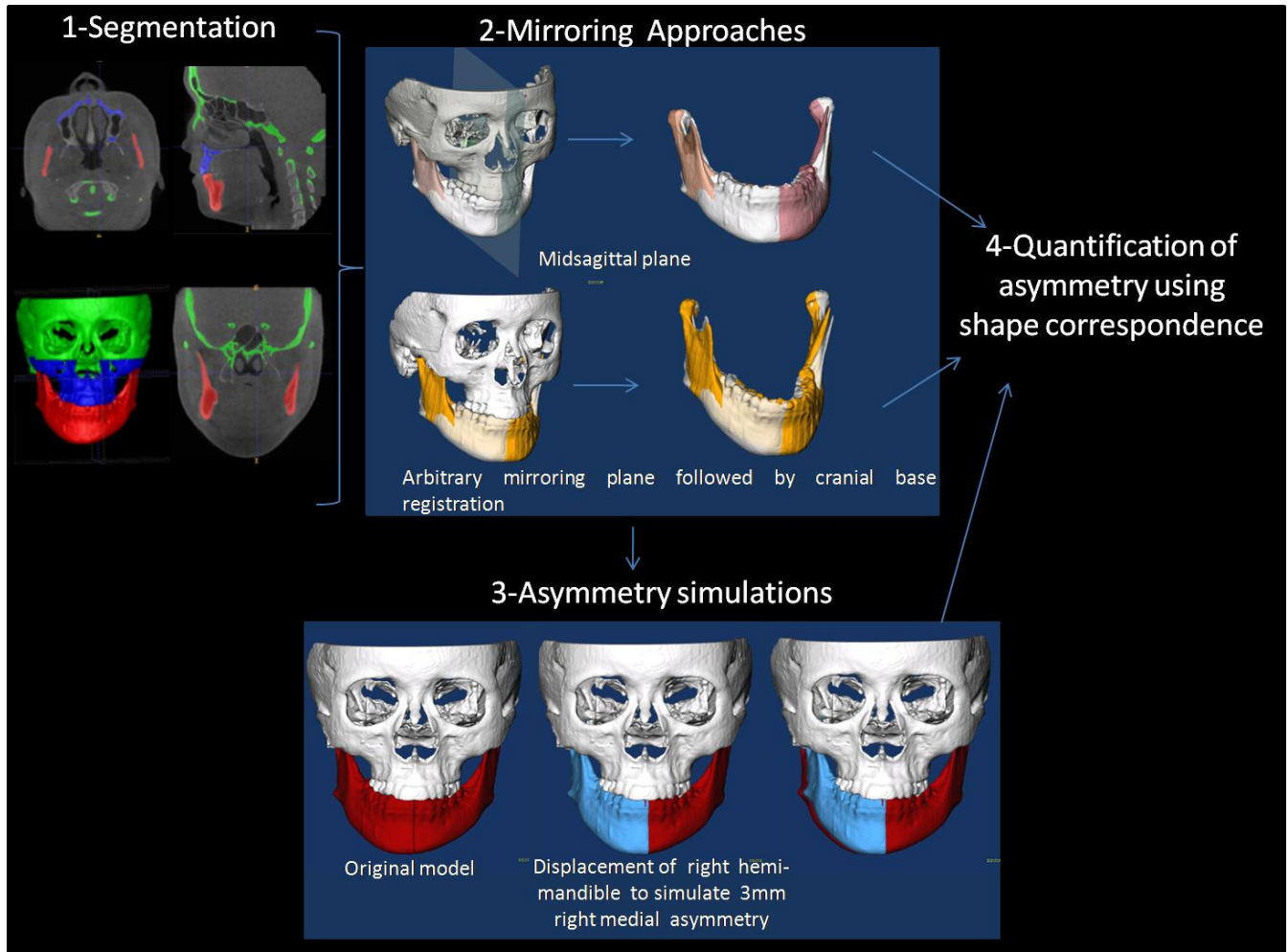


Figure 8. Image segmentation: Cone beam CT images are imported as DICOM files into ITK Snap. In a process known as semiautomatic segmentation anatomical areas of interest are identified and delineated. Manual editing is performed to ensure accuracy of the segmentations. The images can be viewed in three dimensions and as axial, coronal, and sagittal slices of each image.

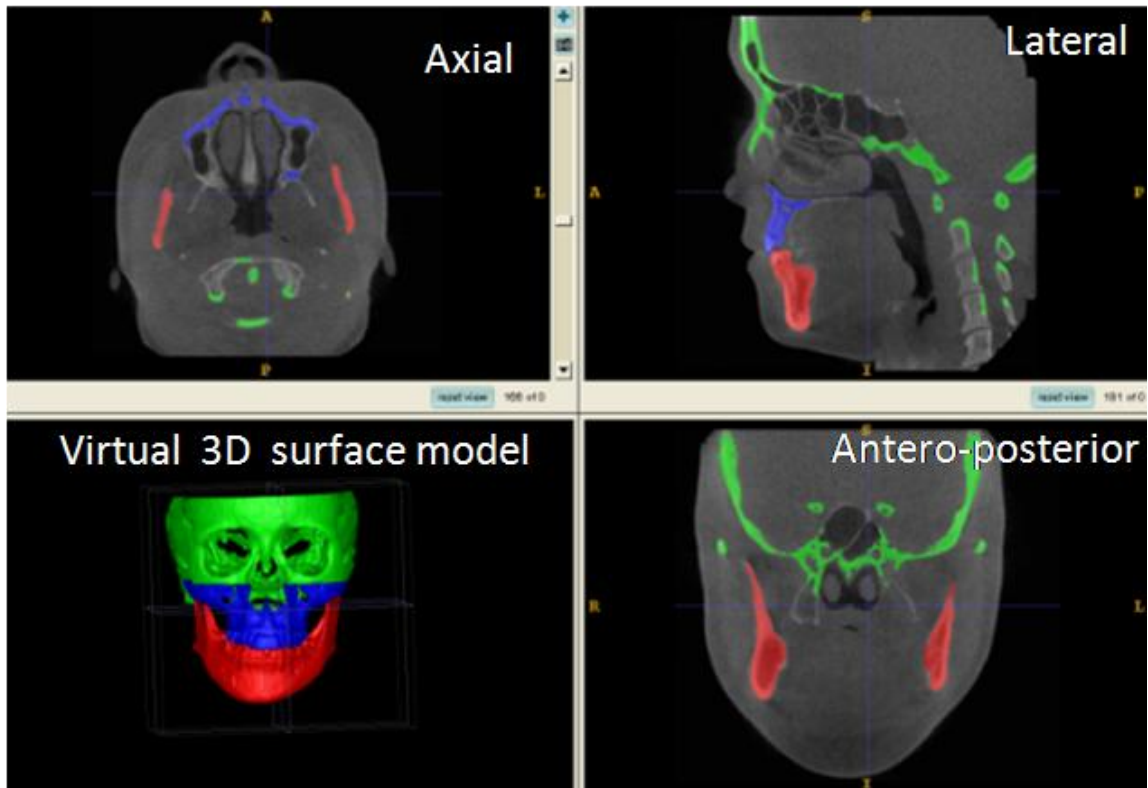


Figure 9. Three-dimensional image mirroring on the midsagittal plane: Mirroring can be a valuable technique in the treatment of asymmetries. As shown below the mandible (A) has been colored yellow. (B) The left ramus was mirrored onto the right side using the CMF applications mirror function and the mid-sagittal plane was defined for the image. (C) The right lateral ramus was then reincorporated back into the model with the right side recreated as a mirror of the left side.

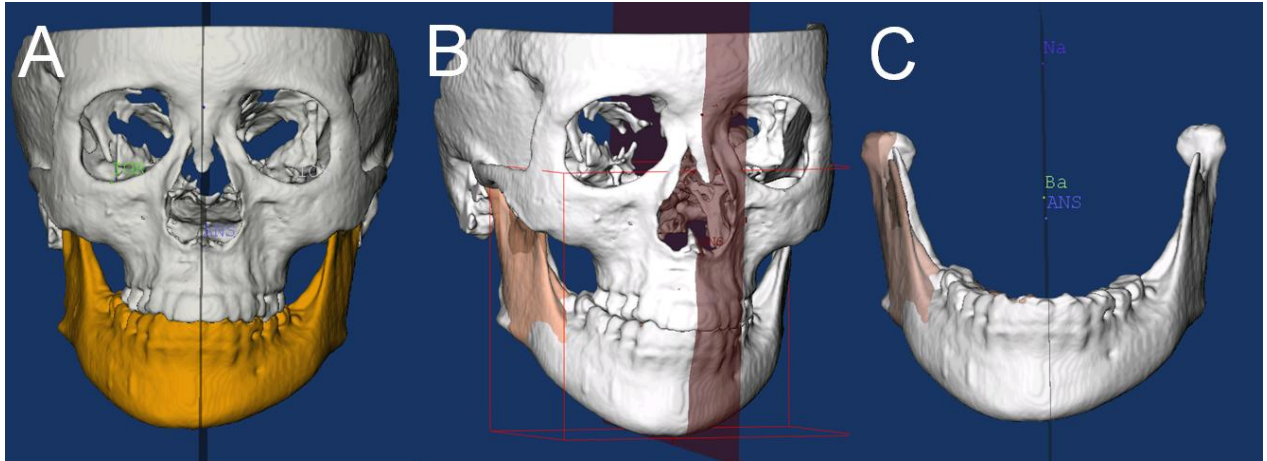


Figure 10. Arbitrary Plane Mirroring followed by Cranial Base Registration Approach

A. Cranial base virtual surface model for a patient (*white*) and arbitrarily mirrored image model (*purple*); B, original model and arbitrary mirror matching on the cranial base as a result of a voxel-based registration; C, color map of the surface distance between the registered original and arbitrary mirror models shown at 0-mm surface distances (*green*); D. Virtual surface model (*white*) and registered arbitrarily mirrored image model (*orange*); E. Close-up showing mandibular asymmetry.

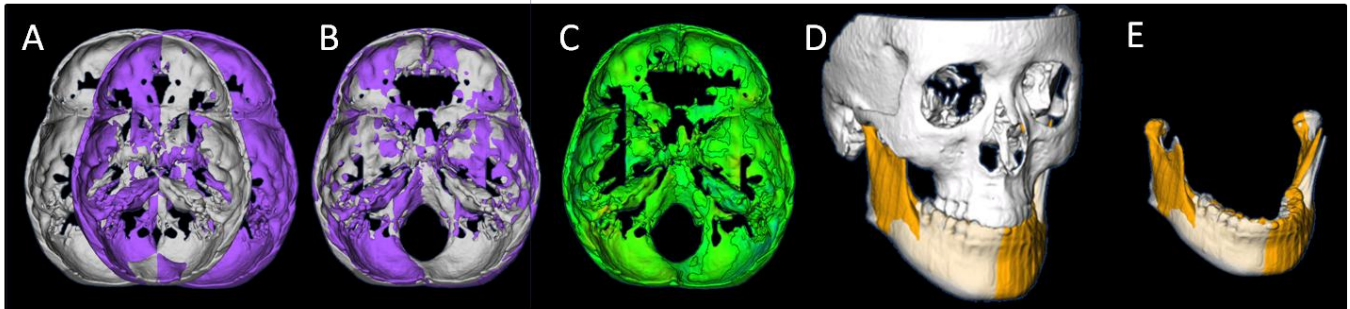


Figure 11. Asymmetry simulation The segmented 3-dimensional surface models of hemimandibles are displaced in the lateral (X axis, yaw) and superior inferior (Z axis, roll) planes of spaces by 1, 2 and 3mm. The 9 different simulations are shown.

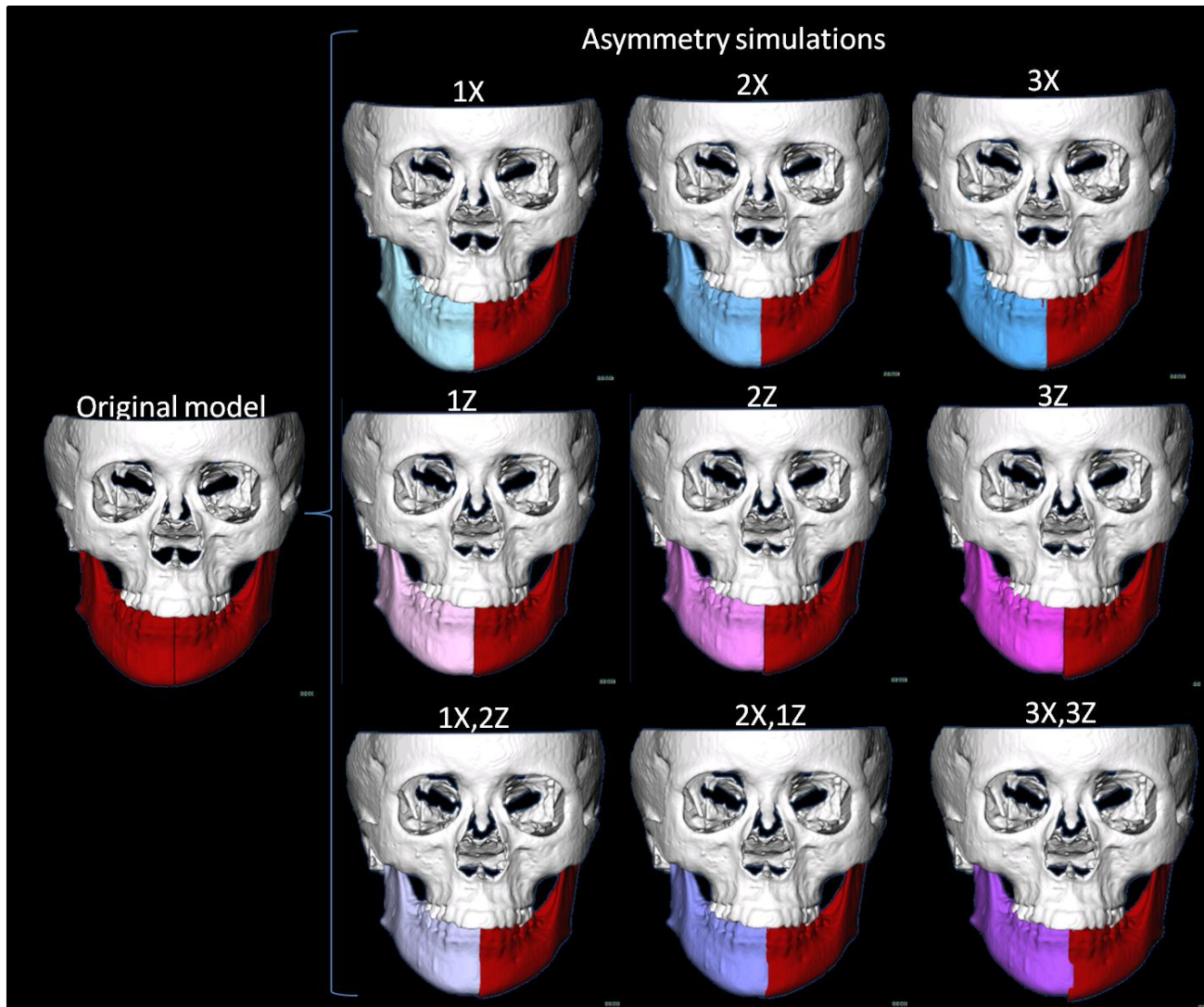


Figure 12. Description of shape correspondence procedures. The segmented 3-dimensional surface models of hemimandibles are converted into surface meshes, and a spherical parametrization is computed for the surface meshes using area-preserving and distortion-minimizing spherical mapping. The SPHARM description is computed from the mesh and its spherical parametrization. Using the first-order ellipsoid from the spherical harmonic coefficients, the spherical parametrizations establish correspondence across all surfaces. The SPHARM description is then sampled into a triangulated surface (SPHARM-PDM). The hemi-mandibles are represented using thousands of surface points. Procrustes alignment is used to compute the differences in the alignment.

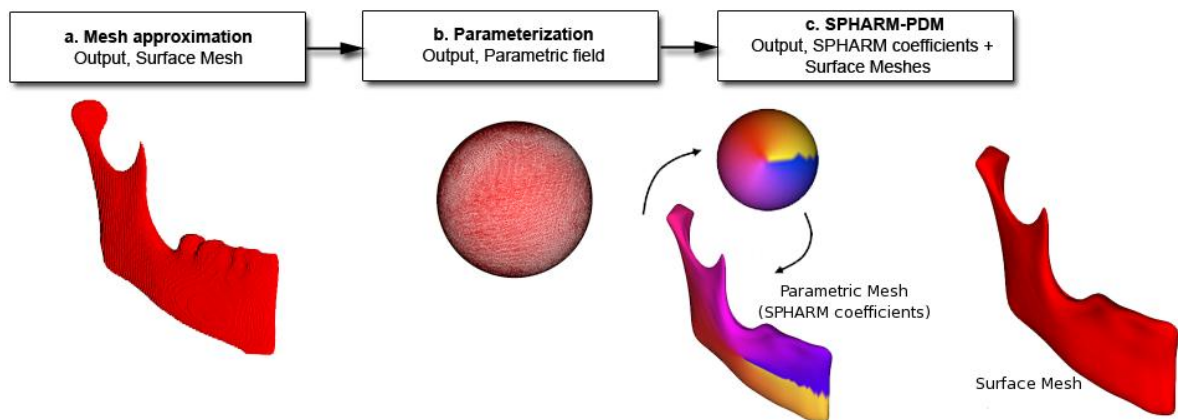


Figure 13. Quantification of mandibular asymmetry for a patient using Shape Correspondence. A, original model (*grey*) and left hemi-mandible arbitrary mirror matching on the cranial base (*maroon*); B, Shape Correspondence can be used to quantify the right and left differences as represented in this vectorial color map of the surface distance between the registered original and arbitrary mirror models; C. Signed color maps showing the directionality of the differences the left ramus is wider and left corpus is narrower than the right.

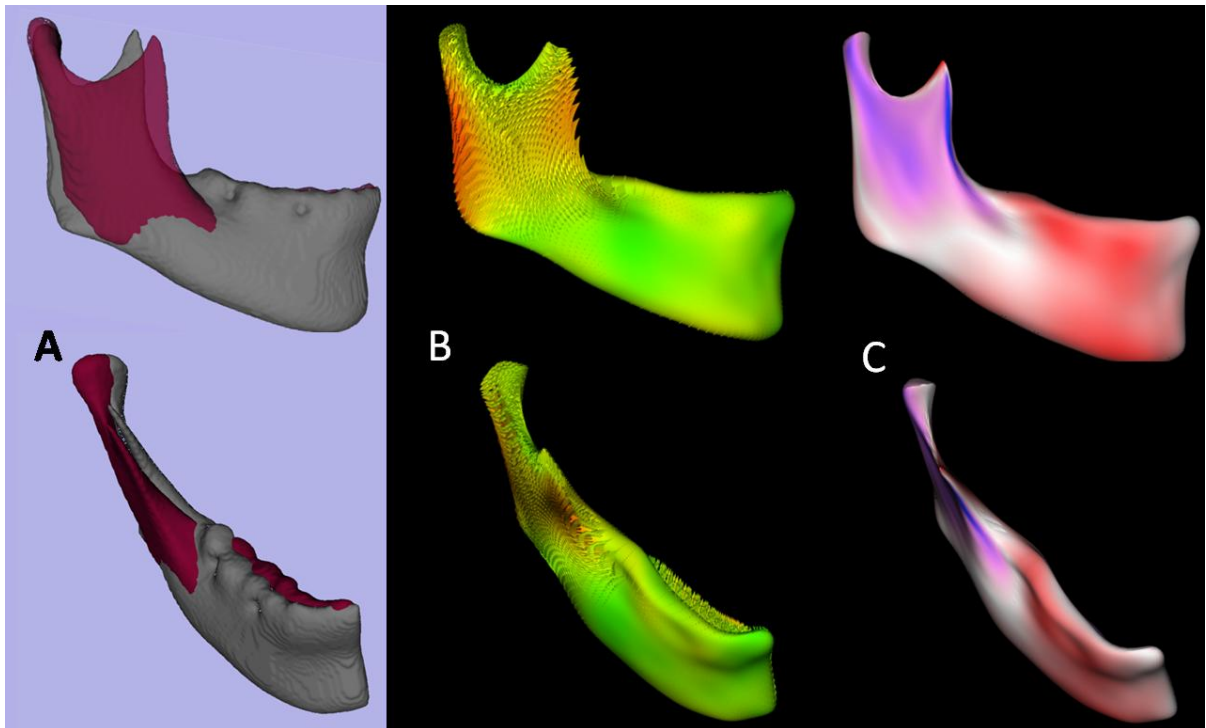


Figure 14. Examples of yaw in mandibular asymmetry. Inferior view of mandibular models for 6 patients. Note that if the asymmetric yaw of the mandibular models is not taken into account, and virtually corrected prior to the use of mirroring techniques, mirroring techniques will yield misleading diagnosis of asymmetry. Asymmetry in the yaw orientation of the mandible would lead to undesirable results if surgical correction corrects chin position with genioplasty but does not properly correct asymmetry in the mandibular corpus and rami.

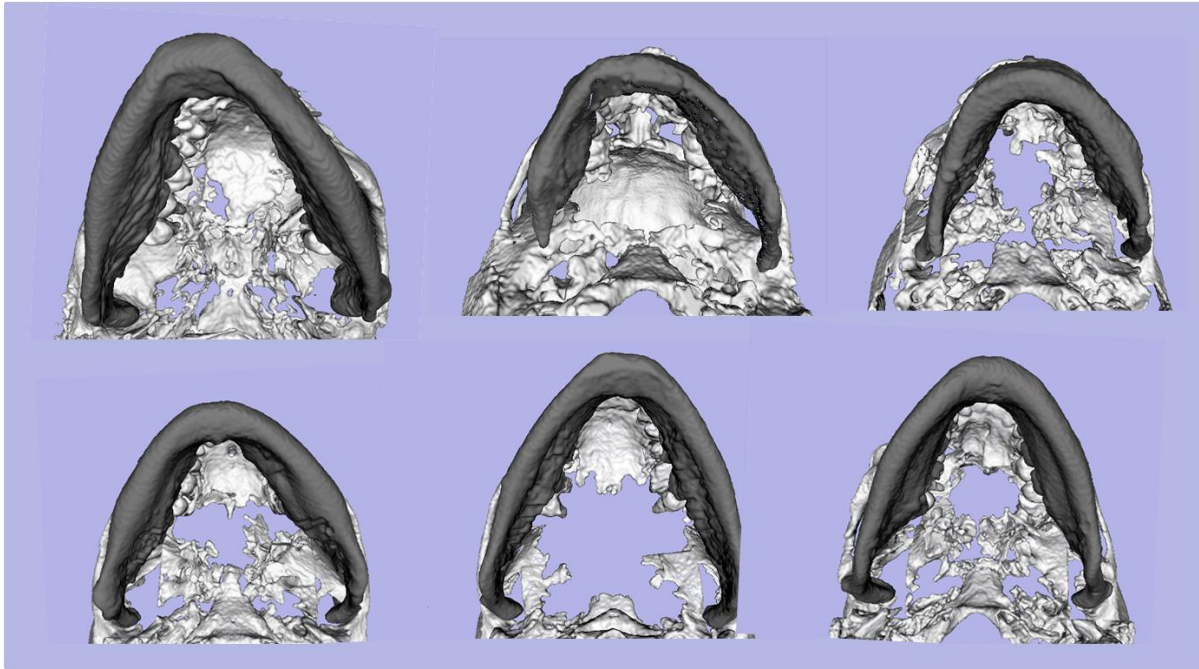


Figure 15. Clinical case 1.



Figure 16. Clinical case 2. Patient's mandible was reoriented before mirroring was executed in an attempt to place the chin in a clinically acceptable location while preserving the facial width. The mandible was rotated 6 degrees anti-clock-wise in frontal plane and 5 degrees clock-wise in axial plane.

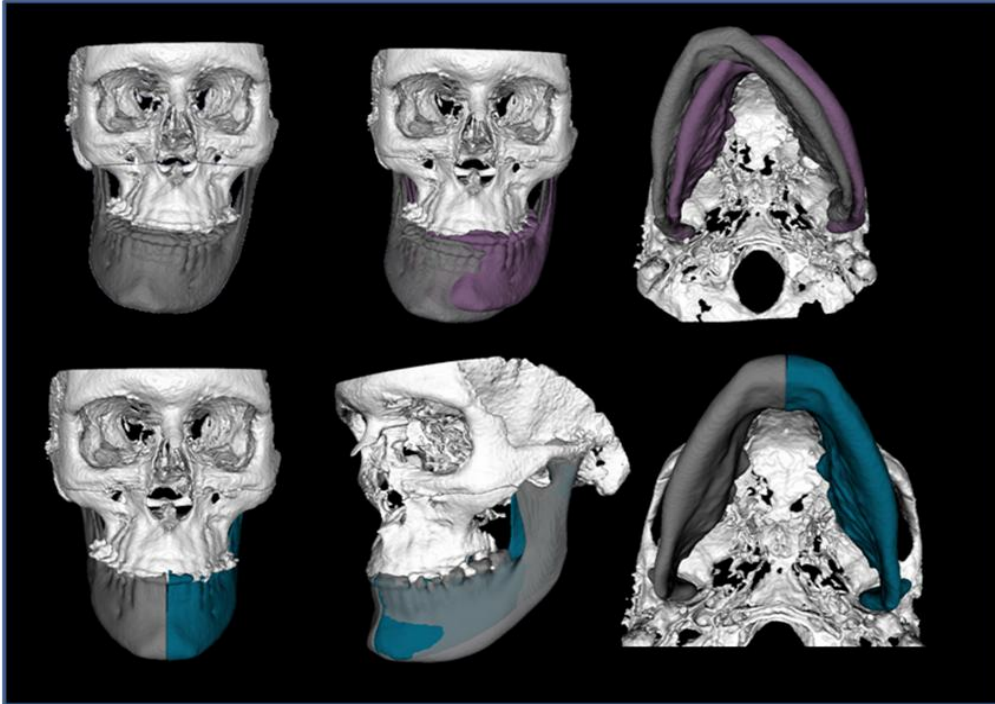


Figure 17. Clinical case 3 Patient's mandible was reoriented before mirroring was executed in an attempt to place the chin in a clinically acceptable location while preserving the facial width. The mandible was rotated 8 degrees clock-wise in the frontal plane using the center of mass as the center of rotation.

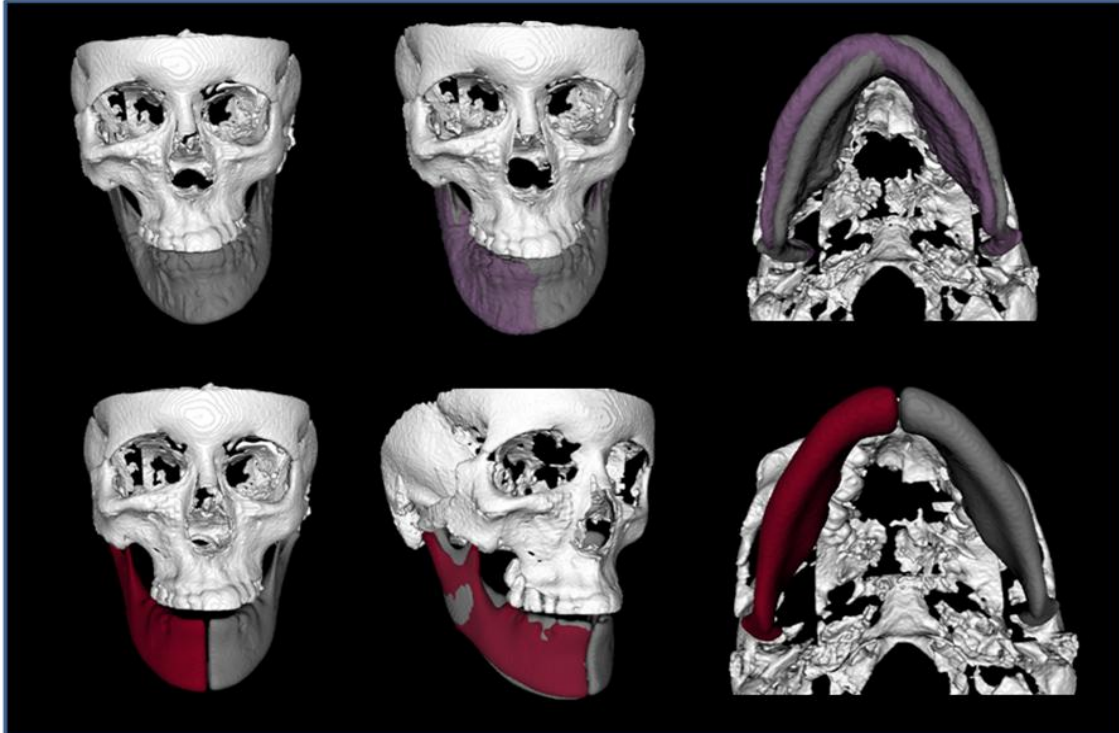


Table 1. Descriptive statistics for the absolute difference in surface distance measurements between the two methods at the different anatomical locations

	N	Mean	Std. Deviation
Lateral pole of the left condyle	47	1.73	1.36
Left Ramus	50	2.00	2.50
Left Body	50	2.14	2.57
Left symphysis	50	2.35	2.27
Left inferior border	50	1.70	1.94
Left Posterior border	50	1.71	1.65
Posterior surface of the left condyle	47	1.53	1.50
Medial surface of the left condyle	47	1.41	1.79
Anterior surface of the left condyle	47	1.35	1.77
Lateral pole of the right condyle	48	1.84	2.18
Right Ramus	50	2.54	3.08
Right body	50	2.82	3.21
Right symphysis	50	2.58	2.34
Right inferior border	50	1.42	1.57
Right posterior border	50	1.48	1.37
Posterior surface of the right condyle	48	1.65	1.90
Medial pole of the right condyle	48	1.62	1.37
Anterior surface of the right condyle	48	1.59	1.87

Table 2. The probabilities, confidence intervals and prediction intervals for each x, y z possible planes of rotation and translation measured for the simulated asymmetries using mirroring in the midsagittal plan2

Midsagittal plane	Known asymmetry simulation	6 degrees of freedom	Mean±SD (mm)	CI(Min-Max)	PI(Min-Max)	P(measured mean-known <.5)
Mirror_translation 1x	0	Rx	0.00±0.00	(0.00-0.01)	(0.00-0.01)	1
	0	Ry	0.01±0.01	(0.00-0.01)	(-0.02-0.03)	1
	0	Rz	0.01±0.01	(0.00-0.01)	(-0.01-0.02)	1
	1	Tx	1.02±0.11	(0.97-1.08)	(0.79-1.26)	1
	0	Ty	0.00±0.01	(0.00-0.01)	(-0.01-0.02)	1
	0	Tz	0.00±0.00	(0.00-0.01)	(0.00-0.01)	1
Mirror_translation 1x_2z	0	Rx	0.01±0.01	(0.00-0.01)	(-0.01-0.03)	1
	0	Ry	0.01±0.01	(0.00-0.01)	(-0.01-0.03)	1
	0	Rz	0.01±0.01	(0.00-0.01)	(-0.01-0.03)	1
	1	Tx	1.03±0.11	(0.97-1.08)	(0.79-1.27)	1
	0	Ty	0.01±0.00	(0.00-0.01)	(-0.01-0.02)	1
	2	Tz	2.00±0.01	(1.99-2.00)	(1.99-2.01)	1
Mirror_translation 1z	0	Rx	0.00±0.00	(0.00-0.01)	(-0.01-0.01)	1
	0	Ry	0.01±0.02	(0.00-0.02)	(-0.02-0.05)	1
	0	Rz	0.01±0.01	(0.00-0.01)	(-0.01-0.03)	1
	0	Tx	0.08±0.34	(-0.08-0.23)	(-0.64-0.80)	0.99
	0	Ty	0.01±0.01	(0.00-0.01)	(-0.01-0.02)	1
	1	Tz	1.00±0.00	(0.99-1.00)	(0.99-1.01)	1
Mirror_translation 2x	0	Rx	0.01±0.01	(0.00-0.01)	(-0.01-0.02)	1
	0	Ry	0.00±0.01	(0.00-0.01)	(-0.01-0.02)	1
	0	Rz	0.00±0.01	(0.00-0.01)	(-0.01-0.02)	1
	2	Tx	1.97±0.11	(1.92-2.03)	(1.73-2.22)	1
	0	Ty	0.00±0.00	(0.00-0.01)	(-0.01-0.01)	1
	0	Tz	0.00±0.00	(0.00-0.01)	(0.00-0.01)	1
Mirror_translation 2x_1z	0	Rx	0.01±0.01	(0.00-0.01)	(-0.01-0.02)	1
	0	Ry	0.01±0.01	(0.01-0.02)	(-0.02-0.04)	1
	0	Rz	0.01±0.01	(0.01-0.02)	(-0.01-0.03)	1
	2	Tx	1.97±0.11	(1.92-2.03)	(1.73-2.21)	1
	0	Ty	0.01±0.01	(0.00-0.01)	(-0.01-0.02)	1
	1	Tz	1.00±0.00	(0.99-1.00)	(0.99-1.01)	1
Mirror_translation 2z	0	Rx	0.01±0.01	(0.00-0.01)	(-0.01-0.02)	1
	0	Ry	0.01±0.01	(0.00-0.01)	(-0.02-0.03)	1
	0	Rz	0.01±0.01	(0.00-0.01)	(-0.01-0.02)	1
	0	Tx	0.08±0.34	(-0.08-0.23)	(-0.64-0.80)	0.99
	0	Ty	0.00±0.01	(0.00-0.01)	(-0.01-0.02)	1
	2	Tz	2.00±0.00	(1.99-2.00)	(1.99-2.01)	1
Mirror_translation 3x	0	Rx	0.01±0.00	(0.00-0.01)	(0.00-0.01)	1
	0	Ry	0.01±0.01	(0.00-0.02)	(-0.02-0.04)	1
	0	Rz	0.01±0.01	(0.00-0.01)	(-0.01-0.02)	1
	3	Tx	2.92±0.34	(2.77-3.08)	(2.21-3.64)	0.99
	0	Ty	0.00±0.01	(0.00-0.01)	(-0.01-0.02)	1
	0	Tz	0.00±0.00	(0.00-0.01)	(-0.00-0.01)	1
Mirror_translation 3x_3z	0	Rx	0.01±0.01	(0.00-0.01)	(-0.01-0.02)	1
	0	Ry	0.01±0.01	(0.00-0.01)	(-0.01-0.02)	1
	0	Rz	0.01±0.01	(0.00-0.01)	(0.00-0.02)	1
	3	Tx	2.92±0.34	(2.77-3.08)	(2.21-2.64)	0.99
	0	Ty	0.00±0.01	(0.00-0.01)	(-0.01-0.02)	1
	3	Tz	3.00±0.00	(2.99-3.00)	(2.99-3.01)	1
Mirror_translation 3z	0	Rx	0.01±0.01	(0.00-0.01)	(-0.01-0.02)	1
	0	Ry	0.01±0.01	(0.00-0.02)	(-0.02-0.04)	1
	0	Rz	0.01±0.01	(0.00-0.01)	(-0.01-0.02)	1
	0	Tx	0.08±0.34	(-0.08-0.24)	(-0.64-0.80)	0.99
	0	Ty	0.01±0.01	(0.00-0.01)	(-0.01-0.02)	1
	3	Tz	3.00±0.00	(2.99-3.00)	(2.99-3.01)	1

Table 3. Same statistics for the arbitrary mirroring/cranial base registrations approach

Cranial base registration	Known asymmetry simulation	6 degrees of freedom	Mean±SD (mm)	CI(Min-Max)	PI(Min-Max)	P(measured mean-known <.5)
Mirror_translation 1x	0	Rx	0.01±0.00	(0.00-0.01)	(-0.01-0.02)	1
	0	Ry	0.01±0.01	(0.00-0.01)	(-0.02-0.03)	1
	0	Rz	0.01±0.01	(0.00-0.01)	(-0.01-0.02)	1
	1	Tx	1.02±0.11	(0.97-1.08)	(0.79-1.26)	1
	0	Ty	0.00±0.01	(0.00-0.01)	(-0.01-0.02)	1
	0	Tz	0.00±0.00	(0.00-0.01)	(0.00-0.01)	1
Mirror_translation 1x_2z	0	Rx	0.01±0.01	(0.00-0.01)	(-0.01-0.03)	1
	0	Ry	0.01±0.01	(0.00-0.01)	(-0.01-0.03)	1
	0	Rz	0.01±0.01	(0.00-0.01)	(-0.01-0.03)	1
	1	Tx	1.03±0.11	(0.97-1.08)	(0.79-1.27)	1
	0	Ty	0.01±0.00	(0.00-0.01)	(-0.01-0.02)	1
	2	Tz	2.00±0.01	(1.99-2.00)	(1.99-2.01)	1
Mirror_translation 1z	0	Rx	0.00±0.00	(0.00-0.01)	(-0.01-0.02)	1
	0	Ry	0.01±0.02	(0.00-0.02)	(-0.02-0.05)	1
	0	Rz	0.01±0.01	(0.00-0.01)	(-0.01-0.03)	1
	0	Tx	0.08±0.34	(-0.08-0.23)	(-0.64-0.80)	0.85
	0	Ty	0.01±0.01	(0.00-0.01)	(-0.01-0.02)	1
	1	Tz	1.00±0.00	(0.99-1.00)	(0.99-1.01)	1
Mirror_translation 2x	0	Rx	0.01±0.01	(0.00-0.01)	(-0.01-0.03)	1
	0	Ry	0.00±0.01	(0.00-0.01)	(-0.01-0.02)	1
	0	Rz	0.00±0.01	(0.00-0.01)	(-0.01-0.02)	1
	2	Tx	1.97±0.11	(1.92-2.03)	(1.73-2.22)	1
	0	Ty	0.00±0.00	(0.00-0.01)	(-0.01-0.01)	1
	0	Tz	0.00±0.00	(0.00-0.01)	(0.00-0.01)	1
Mirror_translation 2x_1z	0	Rx	0.01±0.01	(0.00-0.01)	(-0.01-0.02)	1
	0	Ry	0.01±0.01	(0.01-0.02)	(-0.02-0.04)	1
	0	Rz	0.01±0.01	(0.01-0.02)	(-0.01-0.02)	1
	2	Tx	1.97±0.11	(1.92-2.03)	(1.73-2.21)	1
	0	Ty	0.01±0.01	(0.00-0.01)	(-0.01-0.02)	1
	1	Tz	1.00±0.00	(0.99-1.00)	(0.99-1.01)	1
Mirror_translation 2z	0	Rx	0.01±0.01	(0.00-0.01)	(-0.01-0.02)	1
	0	Ry	0.01±0.01	(0.00-0.01)	(-0.02-0.03)	1
	0	Rz	0.01±0.01	(0.00-0.01)	(-0.01-0.02)	1
	0	Tx	0.08±0.34	(-0.08-0.23)	(-0.64-0.80)	0.85
	0	Ty	0.00±0.01	(0.00-0.01)	(-0.01-0.02)	1
	2	Tz	2.00±0.00	(1.99-2.00)	(1.99-2.01)	1
Mirror_translation 3x	0	Rx	0.01±0.00	(0.00-0.01)	(0.00-0.02)	1
	0	Ry	0.01±0.01	(0.00-0.02)	(-0.02-0.04)	1
	0	Rz	0.01±0.01	(0.00-0.01)	(-0.01-0.02)	1
	3	Tx	2.92±0.34	(2.77-3.08)	(2.21-3.64)	0.85
	0	Ty	0.00±0.01	(0.00-0.01)	(-0.01-0.02)	1
	0	Tz	0.00±0.00	(0.00-0.01)	(-0.00-0.01)	1
Mirror_translation 3x_3z	0	Rx	0.01±0.01	(0.00-0.01)	(-0.01-0.02)	1
	0	Ry	0.01±0.01	(0.00-0.01)	(-0.01-0.02)	1
	0	Rz	0.01±0.01	(0.00-0.01)	(0.00-0.02)	1
	3	Tx	2.92±0.34	(2.77-3.08)	(2.21-3.64)	0.85
	0	Ty	0.00±0.01	(0.00-0.01)	(-0.01-0.02)	1
	3	Tz	3.00±0.00	(2.99-3.00)	(2.99-3.01)	1
Mirror_translation 3z	0	Rx	0.01±0.01	(0.00-0.01)	(-0.01-0.02)	1
	0	Ry	0.01±0.01	(0.00-0.02)	(-0.02-0.04)	1
	0	Rz	0.01±0.01	(0.00-0.01)	(-0.01-0.02)	1
	0	Tx	0.08±0.34	(-0.08-0.24)	(-0.64-0.80)	0.85
	0	Ty	0.01±0.01	(0.00-0.01)	(-0.01-0.02)	1
	3	Tz	3.00±0.00	(2.99-3.00)	(2.99-3.01)	1